Received: 18 March 2022 | Revised: 6 April 2022 | Accepted: 7 April 2022

DOI: 10.1002/bio.4248

RESEARCH ARTICLE

LUMINESCENCE The Journal of Biological and Chemical Luminescence WILEY

A sensitive electrochemiluminescent sensor chip based on the ssDNA-Ru(II) complex and aptamer for the determination of thrombin

Weiwei Luo[1,2] | Zhuoxin Ye[1] | Daqian Song[1] | Pinyi Ma[1]

[1]College of Chemistry, Jilin Province Research Center for Engineering and Technology of Spectral Analytical Instruments, Jilin University, Qianjin Street 2699, Changchun, China

[2]School of Chemistry and Life Science, Anshan Normal University, Ping'an Street 43, Anshan, China

Correspondence
Pinyi Ma, College of Chemistry, Jilin Province Research Center for Engineering and Technology of Spectral Analytical Instruments, Jilin University, Qianjin Street 2699. Changchun, 130012, China.
Email: mapinyi@jlu.edu.cn

Funding information
National Natural Science Foundation of China, Grant/Award Numbers: 22074052, 22004046

Abstract

In this work, an electrochemiluminescence (ECL) sensor chip for sensitive detection of thrombin (TB) was prepared using a screen-printed electrode (SPE) as a working electrode and an aptamer as a specific recognition moiety. To produce an ECL sensor chip, a layer of p*L*-Cys was immobilized on the surface of the SPE using the cyclic voltammetry scanning method. A layer of gold nanoparticles (AuNPs) was assembled through an Au–S bond and hairpin DNA was further immobilized on the electrode surface. $Ru(bpy)_2(mcpbpy)^{2+}$, as a luminescent reagent, was covalently bound to single-stranded DNA (ssDNA) to prepare a luminescence probe ssDNA-Ru. The probe was hybridized with TB aptamer to form a capture probe. In the presence of TB, the TB aptamer in the capture probe bound to TB, causing the release of ssDNA-Ru that could bind to hairpin DNA on the electrode surface. The Ru(II) complex as a luminescent reagent was assembled onto the electrode, and p*L*-Cys was used as a co-reactant to enhance the ECL efficiency. The ECL signal of the sensor chip generated based on the above principles had a linear relationship with log TB concentration at the range 10 fM to1 nM, and the detection limit was 0.2 fM. Finally, TB detection using this method was verified using real blood samples. This work provides a new method using an aptamer as a foundation and SPE as a material for the detection of biological substances.

KEYWORDS
aptamer, electrochemiluminescence (ECL), screen-printed electrode (SPE), sensor chip, thrombin (TB)

1 | INTRODUCTION

Thrombin (TB), a multifunctional serine protease, is a key protein that is involved in the regulation of haemostasis and plays a vital role in various biological processes.[1] It is also involved in many diseases, such as cardiovascular diseases, inflammatory response, and thromboembolic diseases, as well as in hemostatic treatment.[2–4] The currently available TB detection methods include high performance liquid chromatography (HPLC),[5,6] fluorescence spectra,[7–9] surface plasmon resonance (SPR),[10–14] electrochemistry,[15–17] and electrochemiluminescence (ECL).[18–25] Among these methods, ECL is the method widely used in various bioanalyses due to its simplicity, high sensitivity, wide dynamic range, and low background interference.[26]

An aptamer is a single-stranded or double-stranded oligonucleotide fragment obtained from artificially constructed random single-stranded oligonucleotide (ssDNA or ssRNA) libraries through ligand index enrichment phylogenetic evolution technology.[27] Aptamers have an ability to recognize various targets, can be easily prepared, have higher thermal stability and are more controllable.[28] In recent

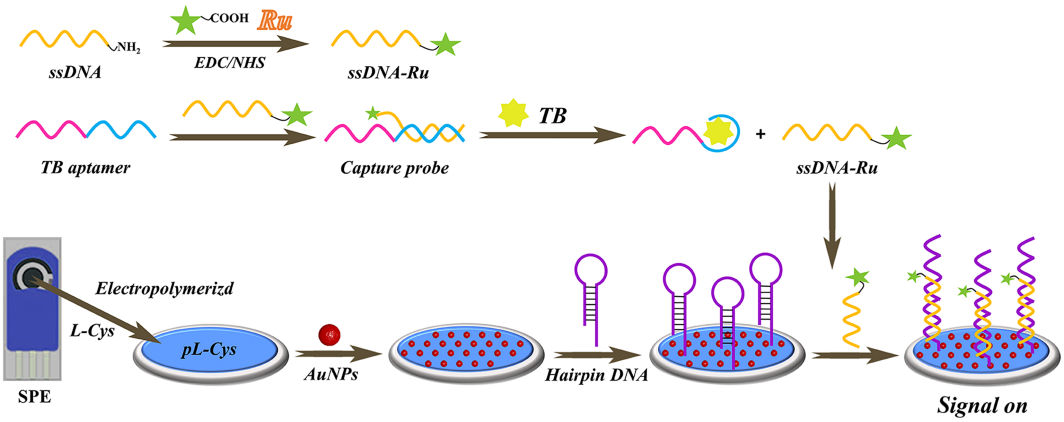

FIGURE 1 Schematic representation showing the detection principle using the prepared ECL sensor chip

years, the use of aptamers as molecular recognition moieties has attracted considerable attention from researchers.[29–32]

Since its first ECL properties were reported by Tokel and Bard,[33] ruthenium bipyridine ($Ru(bpy)_3^{2+}$) has become the most widely studied and applied ECL compound due to its high chemical stability and good redox properties.[34] $Ru(bpy)_3^{2+}$ alone has been reported to have relatively low ECL intensity. However, its luminous efficiency can be significantly improved by introducing a co-reactant into the system.[35,36] In a traditional detection method, a co-reactant is usually added to the luminescent reagent to improve its ECL signal. However, the electron transfer between the luminescent reagent and co-reactant can increase the electron transfer distance and energy loss, which will reduce the luminous efficiency of the luminescent reagent.[37]

In this work, we introduced a screen-printed electrode (SPE) into a biosensor, which is a disposable electrode for rapid and point-of-care detection. Here, we constructed a novel ECL sensor chip for quantitative detection of TB using nucleic acid aptamers as specific recognition moieties, $Ru(bpy)_2(mcpbpy)^{2+}$ as a luminescent reagent, and poly-L-cysteine (p*L*-Cys) as a co-reactant,[38] to combine with an SPE. p*L*-Cys could form the strongly reducing radical of pL-Cys$^{\bullet}$ to improve the ECL efficiency of the luminescent reagent. First, a layer of p*L*-Cys was coated on the surface of the SPE electrode using the cyclic voltammetry scanning method, and to increase the immobilization capacity of the nucleic acid, a layer of gold nanoparticles (AuNPs) was further assembled onto the p*L*-Cys layer through an Au–S bond. Hairpin DNA containing sulfhydryl groups was then immobilized onto the electrode surface to produce an ECL sensor chip. The luminescence probe ssDNA-Ru was prepared by linking $Ru(bpy)_2(mcpbpy)^{2+}$ with ssDNA through an amide bond, and the probe ssDNA-Ru was complementary to a part of the base sequence of the TB aptamer to form a capture probe. In the presence of TB, the aptamer in the capture probe bound to TB, resulting in the dissociation of ssDNA-Ru. After the solution was dropped onto the ECL sensor chip, the hairpin DNA could then form a double strand through complementary base pairing with the free ssDNA-Ru. The electrode coated with luminescent reagent $Ru(bpy)_2(mcpbpy)^{2+}$ and p*L*-Cys (a co-reactant) had a greatly enhanced ECL signal. Therefore, the specific and highly sensitive detection of TB could be observed as the increase in the ECL signal. The schematic diagram illustrating the experimental principle is shown in Figure 1.

2 | EXPERIMENTAL

2.1 | Reagents and instruments

All oligonucleotides used were purchased from Shanghai Sangon Biological Engineering Technology & Services Co., Ltd (Shanghai, China). Their sequences are listed as follows.

TB aptamer: 5′-GGTTGGTGTGGTTGGCCATTTTTT-3′;
ssDNA probe: 5′-NH_2-GACCTTCATC*CAACCACACCAACC*-3′ (italic bases indicate the sequence of the TB aptamer);
hairpin DNA probe: 5′-SH-TTT*GGTTGGTGTGGTTGGATGAAGGTCCC*TCACCTTCATCCAACCACA-3′ (italic bases can be hybridized with the ssDNA probe).

$[Ru(bpy)_2(mcpbpy)]Cl_2$ was purchased from SunaTech Inc. (Suzhou, China). L-Cysteine (*L*-Cys), 1-ethyl-3-(3-dimethylaminopropyl)carbodiimide hydrochloride (EDC), and *N*-hydroxy succinimide (NHS) were purchased from the Aladdin Reagent Corporation (Shanghai, China). Thrombin, bovine serum albumin (BSA), immunoglobulin G (IgG), alpha-fetoprotein (AFP), and carcinoembryonic antigen (CEA) were purchased from Shanghai Yuanye Bio-Technology Co., Ltd. Hexyl mercaptan (HT) was purchased from Energy Chemical (Shanghai, China). The SPE was customized by Qingdao Poten Technology Co., Ltd (Qingdao, China), and integrated with three electrodes including a working electrode (carbon), a counterelectrode (carbon), and a reference electrode (Ag/AgCl). All chemical reagents were of analytical grade and used without further purification. Phosphate-buffered solution (PBS; 0.1 M, pH 7.4) was prepared from Na_2HPO_4 (0.1 M), KH_2PO_4 (0.1 M), and KCl (0.1 M). Tris–HCl buffered solution (Tris–HCl, 10 mM, pH 8.0) was prepared from EDTA (1 mM), NaCl

(0.1 M), Tris (10 mM), and HCl. Human serum samples were from China–Japan Union Hospital of Jilin University.

ECL experiments were recorded using a model MPI-A ECL analyzer with wavelength range 300–650 nm (Xi'an Remex Analysis Instruments Co., Ltd, China). Cyclic voltammetry (CV) and electrochemical impedance spectroscopy (EIS) experiments were monitored using a CHI 760E electrochemical workstation (CH Instruments Ins., China). pH was measured using a pH meter (INESA Scientific, China).

2.2 | Synthesis of luminescence probe ssDNA-Ru

First, 4 mg of $[Ru(bpy)_2(mcpbpy)]Cl_2$ were dissolved in 8 ml of PBS solution. Next, 2 ml of a mixed solution containing 160 mg of EDC and 40 mg of NHS was added, the mixture was stirred at room temperature for 2 h. Subsequently, 1.6 ml of 1 μM ssDNA solution was added, and the mixture was further stirred for 12 h. After that, the above solution was precipitated with 0.8 ml of 3 M sodium acetate and 16 ml of ethanol at −20°C for 12 h and was then centrifuged at 12,000 rpm for 30 min. The precipitate was washed twice with cold 70% ethanol and then lyophilized in a vacuum to obtain ssDNA-Ru. Finally, 1 μM of ssDNA-Ru was dissolved in PBS (0.1 M, pH 7.4) and then stored in a refrigerator at 4°C until subsequent use.

2.3 | Pretreatment of DNA

Hairpin DNA was dissolved in Tris–HCl solution to a concentration of 20 μM. Next, the hairpin DNA was annealed at 95°C for 5 min using a polymerase chain reaction (PCR) machine and the solution was cooled down to room temperature. The mixture was then incubated at 37°C for 30 min to obtain the hairpin structure.

2.4 | Preparation of ECL sensor chip

The pretreated screen-printed electrodes[39] were immersed in 20 mM *L*-Cys solution. The potential range of the electrode was set at −0.5−1.0 V, the scanning speed was set to 0.1 V/s, and the CV scanning was carried out six times. A dense layer of p*L*-Cys film was modified on the surface of the electrode. After washing with ultrapure water, the modified electrode was added dropwise with 100 μl of AuNPs with a size of 50 nm (reducing $HAuCl_4$ with citrate) and then incubated at 4°C for 8 h. After rinsing with ultrapure water, the electrode was added dropwise with 10 μl of 1 μM hairpin DNA and dried at 37°C. Finally, after 10 μl of 1 mM HT was added dropwise, the electrode was incubated at room temperature for 1 h.

2.5 | Detection of TB

First, 10 μl of a mixture containing 1 μM ssDNA-Ru and 1 μM TB aptamer (10 μl) were annealed at 95°C for 10 min and stabilized at 4°C for 2 h in a PCR instrument to obtain the hybrid of the two components. Then, TB at different concentrations was reacted with the hybrid at 37°C for 1 h, followed by the ssDNA-Ru chain. Finally, 10 μl of the reaction were dropped onto the prepared ECL sensor chip and allowed to react at 37°C for 40 min. After washing with PBS, the electrode was placed in a small beaker containing 10 ml of PBS (0.1 M, pH 7.4) and used for ECL detection. The ECL detection was carried out at a photomultiplier tube (PMT) of 800 V, a scanning range 0.2–1.3 V, and a scanning speed of 0.1 V/s.

3 | RESULTS AND DISCUSSION

3.1 | Electrochemical characterization of ECL sensor chip

As shown in Figure 2a, the change in the electrochemical properties of the electrode surface during the preparation of the sensor was measured through the CV change of the modified electrode. As can be seen in the figure, the bare SPE exhibited a pair of redox peaks of $Fe(CN)_6^{4-/3-}$. After the electrode was modified with p*L*-Cys, the redox peak current decreased because the p*L*-Cys film could hinder the transport of electrons. When AuNPs were introduced through an Au–S bond, the redox peak current was further increased due to the superior electrical conductivity of the AuNPs, which could help to facilitate the electron transport. After hairpin DNA was added, the current was further decreased significantly. This was due to that the phosphate groups on the main chain of hairpin DNA, which are negative charged, could repel $Fe(CN)_6^{4-/3-}$ and hinder the electron transfer on the electrode surface. The electrospray ionization (ESI) spectra were also measured using the electrode at different states, and the results are shown in Figure 2(b). The impedance of the bare electrode was low but, after being modified with p*L*-Cys film, the impedance increased. After introducing AuNPs, the diameter of the impedance spectrum was significantly decreased, probably due to the good electron transport ability of AuNPs and the increase in the specific surface area of the electrode. After being assembled with the hairpin DNA, the impedance value was further increased due to the formation of an insulating layer on the electrode surface. The above results indicated that the ECL sensor chip was successfully prepared.

3.2 | Characterization of PCR amplicons using polyacrylamide gel electrophoresis

To confirm that the TB detection was based on PCR amplification triggered by the aptamer, polyacrylamide gel electrophoresis (PAGE) experiments were conducted; and the results are shown in Figure 3. Lane 1 shows the DNA marker, the number of bases is 25–500. ssDNA (lane 2) and TB aptamer (lane 3) appeared as single bands. When ssDNA was mixed with the TB aptamer (lane 4), a new bright band appeared, which was the hybridization product of ssDNA and the TB aptamer. Whereas, when TB was added to the hybridization

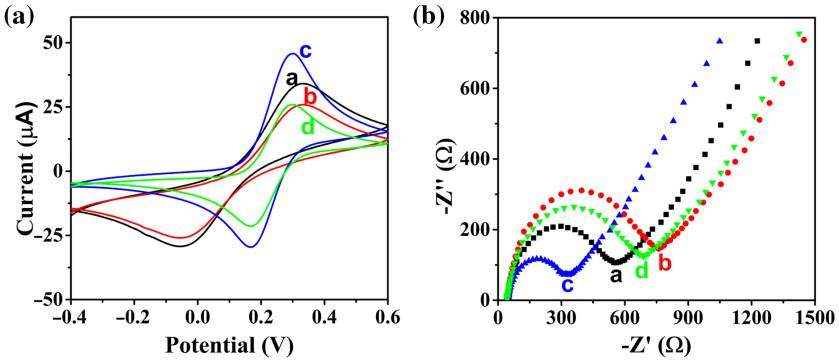

FIGURE 2 CV (a) and EIS (b) of modified SPE in 0.1 M KCl solution containing 5 mM $[Fe(CN)_6]^{3-/4-}$. (Curve a): Bare SPE. (Curve b): SPE/p*L*-Cys. (Curve c: SPE/p*L*-Cys/AuNPs. (Curve d): SPE/p*L*-Cys/AuNPs/hairpin DNA

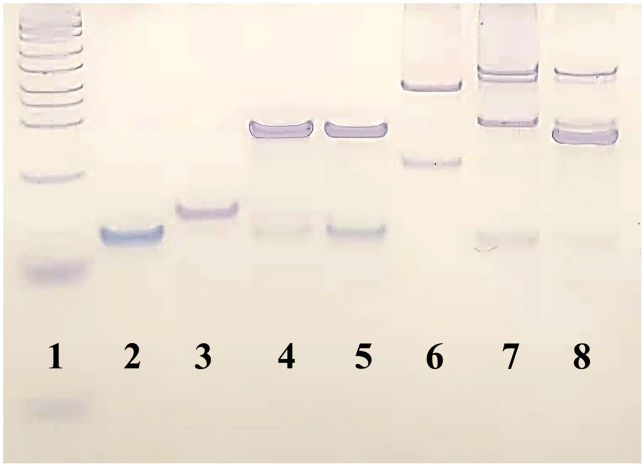

FIGURE 3 PAGE analysis of different samples. Lane 1: marker; lane 2: ssDNA (2 μM); lane 3: TB aptamer (2 μM); lane 4: ssDNA + TB aptamer (both 2 μM); lane 5: ssDNA + TB aptamer + TB (all 2 μM); lane 6: hairpin DNA (2 μM); lane 7: ssDNA + hairpin DNA (both 2 μM); lane 8: ssDNA + TB aptamer + hairpin DNA (all 2 μM)

product of ssDNA and TB aptamer (lane 5), a new band emerged, which was ssDNA, demonstrating the successful release of ssDNA. Lane 6 shows hairpin DNA, in which the low band represents hairpin DNA, which was modified with sulfhydryl groups. Disulfide bonds were formed between sulfhydryl groups, leading to the connection between hairpins to form a high band. The highest band in lane 7 and 8 was also due to the disulfide bond formed by hairpins. Lane 7 was the hybridization products of ssDNA and hairpin DNA. With hairpin DNA added to the hybridization product of ssDNA and TB aptamer (lane 8), hairpin DNA and ssDNA have almost no hybridization, indicating that ssDNA would not be released to hybridize with hairpin DNA when there was no TB, that is, there was no false-positive signal. Based on the above analysis, the proposed strategy was feasible.

3.3 | ECL performance characterization

To evaluate the ECL performance of the SPE electrode, we carried out three comparative experiments. The ssDNA-Ru was used as the target to investigate the ECL performance of four different electrodes: (a) ssDNA-Ru was directly added to SPE (SPE/ssDNA-Ru); (b) SPE was modified with p*L*-Cys before ssDNA-Ru was added (SPE/p*L*-Cys/ssDNA-Ru); (c) SPE was modified with pL-Cys and then directly immobilized with hairpin DNA before ssDNA-Ru was added (SPE/p*L*-Cys/hairpin DNA/ssDNA-Ru); and (d) SPE was modified with pL-Cys, followed by AuNPs and hairpin DNA before ssDNA-Ru was added (SPE/p*L*-Cys/AuNPs/hairpin DNA/ssDNA-Ru) (Figure 4a). The ECL signal of electrode (a) was very weak. The electrode (b) had significantly enhanced signal after being modified with p*L*-Cys, which proves that p*L*-Cys plays a role as a co-reaction promoter. After hairpin DNA was immobilized on the electrode (c), the ECL signal of the electrode was increased, an indication that the hairpin DNA plays a role as a fixer on the electrode surface, causing the number of the binding sites between ssDNA-Ru and the electrode surface to increase. As both p*L*-Cys and hairpin DNA contain S bonds, AuNPs were introduced to modify the electrode (d). On the one hand, the introduction of AuNPs could increase the electrical conductivity of the electrode and improve the electron transport efficiency. On the other hand, more hairpin DNA could be immobilized on the electrode surface, therefore enhancing the sensitivity of the electrode as well as the stability of the assembled material.

According to published literature,[38] we proposed a possible luminescence mechanism of the probe as follows:

$$pL-Cys-e^- \rightarrow pL-Cys^{+\bullet}$$

$$pL-Cys^{+\bullet} \rightarrow pL-Cys^{\bullet} + H^+$$

$$ssDNA-Ru(II)-e^- \rightarrow ssDNA-Ru(III)$$

$$pL-Cys^{\bullet} + ssDNA-Ru(III) \rightarrow ssDNA-Ru(II)^* + pL-Cys^+$$

$$ssDNA-Ru(II)^* \rightarrow ssDNA-Ru(II) + h\nu$$

3.4 | Optimization of experimental conditions

To achieve the highest possible detection sensitivity, we optimized three parameters that were important for experiments, including the

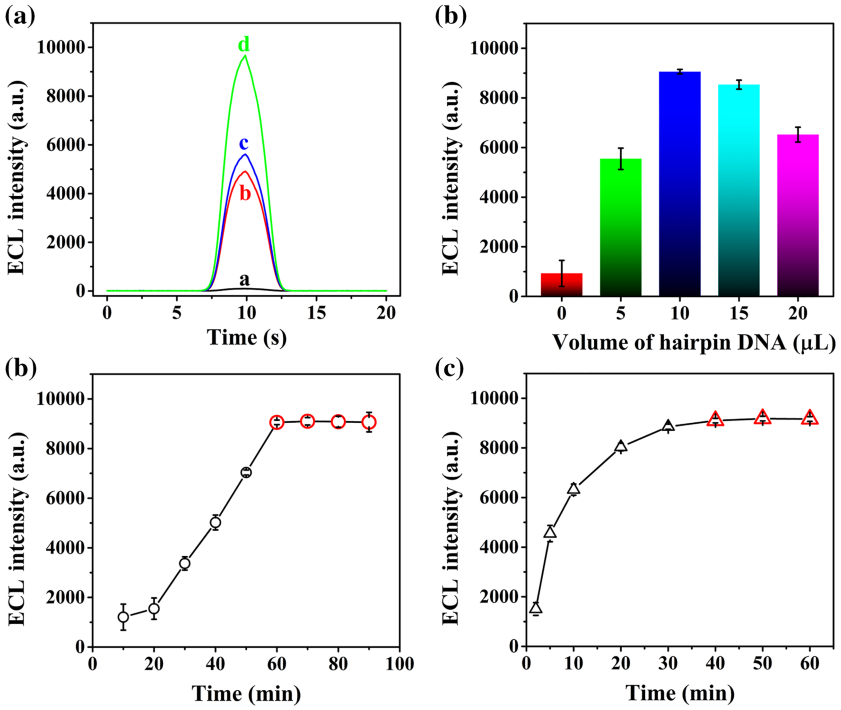

FIGURE 4 (a) ECL response in 0.1 M PBS (pH 7.4). (Curve a): SPE/ssDNA-Ru. (Curve b): SPE/pL-Cys/ssDNA-Ru. (Curve c): SPE/pL-Cys/hairpin DNA/ssDNA-Ru. (Curve d): SPE/pL-Cys/AuNPs/hairpin DNA/ssDNA-Ru. (b) Variation of ECL intensity of 1 μM hairpin DNA with different volumes. (c) Dependence of the ECL intensity of ECL sensor chip on reaction time between the capture probe and TB. (d) Dependence of the ECL intensity of the ECL sensor chip on incubation time between the reaction solution and the auxiliary probe

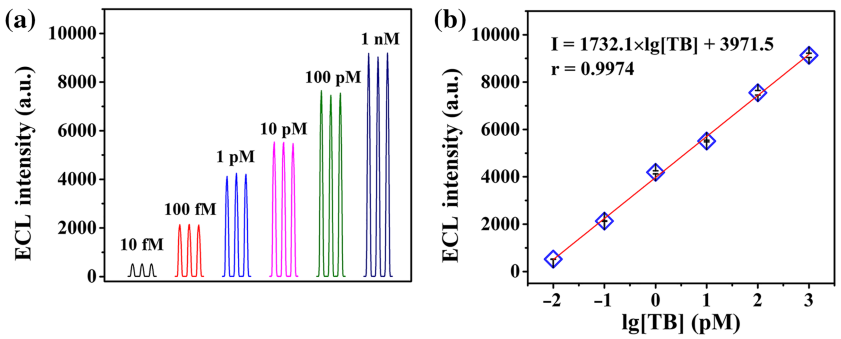

FIGURE 5 (a) Response of ECL biosensor in the presence of TB at different concentrations. (b) Calibration curve of TB determination

content of auxiliary probe hairpin DNA, the reaction time between the capture probe and TB, and the incubation time between the reaction solution and the ECL sensor chip.

First, we investigated the effect of the content of auxiliary probe hairpin DNA on the luminescence properties. Although the increase of hairpin DNA amount could capture more luminescent reagents, its high insulation could also hinder the electron transfer on the electrode surface. Therefore, the concentration of hairpin DNA was also optimized. As shown in Figure 4(b), 10 μl of the 1 μM hairpin DNA was selected as the optimal amount.

We further investigated the effects of reaction time between the capture probe and TB and the incubation time between the reaction solution and the auxiliary probe on the performance of the ECL sensor chip. As can be seen in Figure 4(c, d), the optimal reaction time was 1 h, and the optimal incubation time was 40 min.

3.5 | TB detection using the proposed ECL sensor chip

Figure 5 shows the ECL response diagram and standard curve of the ECL sensor chip under the optimal conditions. According to the result, the intensity of the ECL sensor chip increased with the increase of log TB concentration, and the relationship of the two parameters was linear at the TB concentration range 10 fM to 1 nM. The linear equation for the relationship was $I = 1732.1 \times \lg[TB/(pM)] + 3971.5$ with a correlation coefficient $r = 0.9974$ and a detection limit of 0.2 fM (S/N = 3). The comparison between the present method and other reported TB detection methods is shown in Table 1. As can be seen, the present TB detection method had a wider detection range and lower detection limit. Compared with other ECL methods, we used disposable SPE electrodes to avoid tedious pretreatment steps, which

TABLE 1 Comparison of different methods used for the detection of TB

Methods	Strategies/materials	Detection range	Limit of detection (LOD)	Reference
SERS	Double-aptamer sandwich strategy on plasmonic magnetic beads	20 to 400 pM	30 pM	[40]
Fluorescence	Polymer nanoparticles containing the luminol–terbium (III) complex	0.01 to 25 nM	3.5 pM	[41]
Fluorescence	MNPs@Apt15–thrombin–DC@AuNP sandwich structure	1 to 100 pM	0.78 pM	[42]
Electrochemistry	Highly loaded haemoglobin spheres-encapsulated platinum nanoparticles	0.15 pM to 40 nM	0.05 pM	[43]
ECL	RuNP/PEI-GO-TBA2/PDA/TB-TBA1-PI5CA/Au/GCE	100 fM to 10 nM	28.73 fM	[44]
ECL	$ZnGa_2O_4$/g-C3N4/GCE	1.37 fM to 27.4 pM	0.55 fM	[45]
ECL	SPE/pL-Cys/AuNPs/Hairpin DNA/ssDNA-Ru	10 fM to 1 nM	0.2 fM	This work

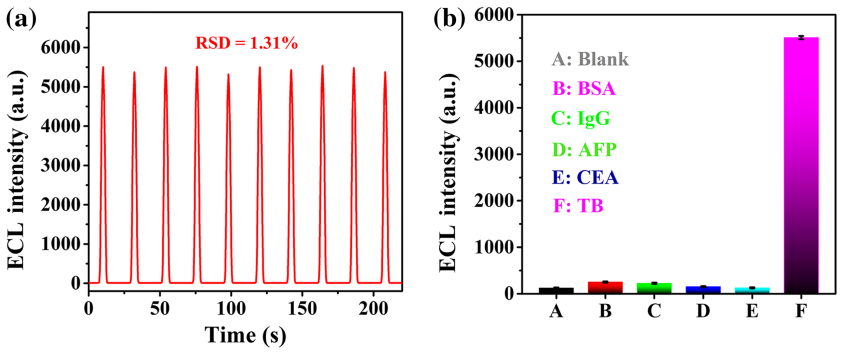

FIGURE 6 (a) Stability of the ECL signal after being subjected to continuous scanning for 10 cycles. (b) Selectivity of the ECL sensor chip towards TB in the presence of each of interfering substances

TABLE 2 Detection of TB in human serum samples using the ECL sensor chip ($n = 3$)

Content of TB (pM)	Spiked (pM)	Detected (pM)	Recovery (%)	RSD
None	1.0	0.97	97.1	4.6%
None	10.0	9.82	98.2	2.2%
None	100.0	95.6	95.6	5.5%
None	500.0	502.8	100.6	7.1%

make our sensor simple, and more repeatable than glassy carbon electrodes (GCE), and could be used for rapid detection.

3.6 | Performance of ECL sensor chip

We selected 10 pM of TB as the object for investigation. We found that the ECL signal was not obviously changed under a continuous scanning for 10 cycles with relative standard deviations (RSDs) of less than 1.31% (Figure 6a). This suggests that the ECL sensor chip had high stability. The RSDs of SPEs from different batches were less than 10%, indicating that the sensor chip had relatively high reproducibility. To evaluate the selectivity of the sensing system, several commonly used proteins, such as BSA (1000 pg/ml), IgG (1000 pg/ml), AFP (50 pM), and CEA (50 pM), were used as interferences during the detection (Figure 6a). The ECL signal intensity of all proteins was not different from that of the blank. By contrast, the ECL signal of the sample in the presence of TB was significantly increased, indicating that the sensor chip had high selectivity towards TB.

3.7 | Detection of TB in human serum

To further evaluate the ability of ECL biosensor to detect TB in complex samples, the proposed method was applied to detect human serum samples. As listed in Table 2, the recovery rates were between 95.6% and 100.6% with RSD values of less than 7.1%. This indicates that the proposed method could accurately and satisfactorily detect TB in human serum samples, and therefore may be suitable for use in the clinical diagnosis of TB.

4 | CONCLUSIONS

In summary, a novel ECL sensor chip for TB detection with high sensitivity was successfully constructed using electro-polymerized pL-Cys as a $Ru(bpy)_2(mcpbpy)^{2+}$ co-reactant, an aptamer with specific recognition ability, and a versatile SPE electrode. The sensor chip was developed using a simple preparation method and could successfully detect TB. It also had a wide linear range, a low detection limit, high

selectivity, and good stability and reproducibility. The present sensor chip may be developed and applied as a tool in the analysis and detection fields, especially in clinical diagnosis.

DECLARATION OF COMPETING INTERESTS

The authors declare that they have no known competing financial interests or personal relationships that could have appeared to influence the work reported in this paper.

ACKNOWLEDGEMENTS

This work was supported by the National Natural Science Foundation of China (Grant Nos. 22004046 and 22074052).

AUTHOR CONTRIBUTIONS

Weiwei Luo: conceptualization, data curation, formal analysis, investigation, writing original draft. Zhuoxin Ye: data curation, investigation, writing original draft. Daqian Song: investigation, resources, writing review. Pinyi Ma: conceptualization, project administration, data curation, writing review and editing, funding acquisition, resources, supervision.

ORCID

Pinyi Ma https://orcid.org/0000-0002-3230-4928

REFERENCES

[1] A. Tripodi, *Clin. Chem.* **2016**, *62*, 699.
[2] J. B. Larsen, A.-M. Hvas, *Semin. Thromb. Hemost.* **2021**, *47*, 759.
[3] F. Depasse, N. B. Binder, J. Mueller, T. Wissel, S. Schwers, M. Germer, B. Hermes, P. L. Turecek, *J. Thromb. Haemost.* **2021**, *19*, 2907.
[4] N. B. Binder, F. Depasse, J. Mueller, T. Wissel, S. Schwers, M. Germer, B. Hermes, P. L. Turecek, *J. Thromb. Haemost.* **2021**, *19*, 2918.
[5] Y. Qiao, Y. Shi, C. Wu, X. Hou, X. Pan, Z. Deng, S. Wang, *J. Sep. Sci.* **2021**, *44*, 3061.
[6] Y. Shi, W. Sun, X. Pan, X. Hou, S. Wang, J. Zhang, *J. Chromatogr. B* **2020**, *1139*, 121894.
[7] T. T. Bezuneh, T. H. Fereja, S. A. Kitte, H. Li, Y. Jin, *Microchem. J.* **2021**, *160*, 105649.
[8] S. Umrao, V. Jain, Anusha, B. Chakraborty, R. Roy, *Sens. Actuators, B* **2018**, *267*, 294.
[9] Z. Chen, M. Sun, F. Luo, K. Xu, Z. Lin, L. Zhang, *Talanta* **2018**, *178*, 563.
[10] D. Kotlarek, F. Curti, M. Vorobii, R. Corradini, M. Careri, W. Knoll, C. Rodriguez-Emmenegger, J. Dostalek, *Sens. Actuators, B* **2020**, *320*, 128380.
[11] S. Li, D. Zhang, Q. Zhang, Y. Lu, N. Li, Q. Chen, Q. Liu, *Sens. Actuators, B* **2016**, *232*, 219.
[12] H. Chen, F. Qi, H. Zhou, S. Jia, Y. Gao, K. Koh, Y. Yin, *Sens. Actuators, B* **2015**, *212*, 505.
[13] P. He, L. Liu, W. Qiao, S. Zhang, *Chem. Commun.* **2014**, *50*, 1481.
[14] S. H. Baek, A. W. Wark, H. J. Lee, *Anal. Chem.* **2014**, *86*, 9824.
[15] L. Bai, B. Yan, Y. Chai, R. Yuan, Y. Yuan, S. Xie, L. Jiang, Y. He, *Analyst* **2013**, *138*, 6595.
[16] L. Bai, Y. Chai, R. Yuan, Y. Yuan, S. Xie, L. Jiang, *Biosens. Bioelectron.* **2013**, *50*, 325.
[17] L. Bai, R. Yuan, Y. Chai, Y. Yuan, Y. Wang, S. Xie, *Chem. Commun.* **2012**, *48*, 10972.
[18] Y. Yang, L.-Y. Yao, W.-B. Liang, W. Huang, Y.-J. Zhang, J.-L. Zhang, R. Yuan, D.-R. Xiao, *Chem. Commun.* **2021**, *57*, 4323.
[19] W. Huang, G.-B. Hu, W.-B. Liang, J.-M. Wang, M.-L. Lu, R. Yuan, D.-R. Xiao, *Anal. Chem.* **2021**, *93*, 6239.
[20] Q. Huang, F. Luo, C. Lin, J. Wang, B. Qiu, Z. Lin, *Biosens. Bioelectron.* **2021**, *189*, 113374.
[21] Y. Fang, H.-M. Wang, Y.-X. Gu, L. Yu, A.-J. Wang, P.-X. Yuan, J.-J. Feng, *Anal. Chem.* **2020**, *92*, 3206.
[22] J. Ge, C. Li, Y. Zhao, X. Yu, G. Jie, *Chem. Commun.* **2019**, *55*, 7350.
[23] Y. Li, Y. Li, N. Xu, J. Pan, T. Chen, Y. Chen, W. Gao, *Sens. Actuators, B* **2017**, *240*, 742.
[24] G. Jie, L. Tan, Y. Zhao, X. Wang, *Biosens. Bioelectron.* **2017**, *94*, 243.
[25] G. Jie, Z. Lu, Y. Zhao, X. Wang, *Sens. Actuators, B* **2017**, *240*, 857.
[26] F. Du, Y. Chen, C. Meng, B. Lou, W. Zhang, G. Xu, *Curr. Opin. Electrochem.* **2021**, *28*, 100725.
[27] S. Ni, Z. Zhuo, Y. Pan, Y. Yu, F. Li, J. Liu, L. Wang, X. Wu, D. Li, Y. Wan, L. Zhang, Z. Yang, B.-T. Zhang, A. Lu, G. Zhang, *ACS Appl. Mater. Interfaces* **2021**, *13*, 9500.
[28] T. Wang, C. Chen, L. M. Larcher, R. A. Barrero, R. N. Veedu, *Biotechnol. Adv.* **2019**, *37*, 28.
[29] M. Lv, W. Zhou, H. Tavakoli, C. Bautista, J. Xia, Z. Wang, X. Li, *Biosens. Bioelectron.* **2021**, *176*, 112947.
[30] F. Li, Z. Yu, X. Han, R. Y. Lai, *Anal. Chim. Acta* **2019**, *1051*, 1.
[31] P. Rothlisberger, M. Hollenstein, *Adv. Drug Deliv. Rev.* **2018**, *134*, 3.
[32] B. Deng, Y. Lin, C. Wang, F. Li, Z. Wang, H. Zhang, X.-F. Li, X. C. Le, *Anal. Chim. Acta* **2014**, *837*, 1.
[33] N. E. Tokel, A. J. Bard, *J. Am. Chem. Soc.* **1972**, *94*, 2862.
[34] V. Balzani, P. Ceroni, A. Credi, M. Venturi, *Chem. Rev.* **2021**, *433*, 213758.
[35] A. Abdussalam, G. Xu, *Anal. Bioanal. Chem.* **2022**, *414*, 131.
[36] L. Chen, J. Wei, Y. Chi, S.-F. Zhou, *ChemElectroChem* **2019**, *6*, 3878.
[37] T. Irkham, A. Watanabe, G. Fiorani, F. Valenti, Y. E. Paolucci, *J. Am. Chem. Soc.* **2016**, *138*, 15636.
[38] Y. L. Yuan, L. Zhang, H. J. Wang, Y. Q. Chai, R. Yuan, *Anal. Chim. Acta* **2018**, *1001*, 112.
[39] W. Luo, H. Chu, X. Wu, P. Ma, Q. Wu, D. Song, *Talanta* **2022**, *239*, 123083.
[40] L. Liao, S. Du, Y. Ding, M. Su, T. Yu, T. Duan, Q. Li, S. He, H. Wang, H. Liu, *Anal. Methods* **2021**, *13*, 4328.
[41] Y. J. Tong, A. M. Song, L. D. Yu, R. P. Liang, J. D. Qiu, *Microchim. Acta* **2020**, *187*, 53.
[42] T. Wu, Y. F. Zhang, T. T. Hou, Y. H. Zhang, S. H. Wang, *Anal. Methods* **2018**, *10*, 4178.
[43] Y. M. Wu, W. J. Xu, L. J. Bai, Y. L. Yuan, H. Y. Yi, Y. Q. Chai, R. Yuan, *Biosens. Bioelectron.* **2013**, *50*, 50.
[44] C. Yang, Y. Tian, B. Wang, Q. Guo, G. Nie, *Sens. Actuators, B* **2021**, *338*, 129870.
[45] H. Liu, H. Yin, T. Yang, H. Ding, Y. Dong, *Analyst* **2020**, *145*, 7412.

How to cite this article: W. Luo, Z. Ye, D. Song, P. Ma, *Luminescence* **2022**, *37*(6), 980. https://doi.org/10.1002/bio.4248